

Improving the Closed-Loop Tracking Performance Using the First-Order Hold Sensing Technique with Experiments

Chifu Yang¹, Shuang Gao², Zhu Xue³

¹Harbin Institute of Technology, Harbin, 150006, China

²McGill University, Montreal, Quebec, H3A 0E9, Canada

³National University of Singapore, 117576, Singapore

Abstract

This paper proposes a new perspective in the enhancement of the closed-loop tracking performance by using the first-order hold (FOH) sensing technique. Firstly, the literature review and fundamentals of the FOH are outlined. Secondly, the performance of the most commonly used zero-order hold (ZOH) and that of the FOH are compared. Lastly, the detailed implementation of the FOH on a pendulum tracking setup is presented to verify the superiority of the FOH over the ZOH in terms of the steady state tracking error. The results of the simulation and the experiment are in agreement.

Keywords: First-order hold, Zero-order hold, Tracking performance, Sensing technique, Pendulum experiment

1. Introduction

The first-order-hold (FOH) method is a mathematical model to reconstruct the sampled signals that could be done by a conventional digital-to-analog converter (DAC) and an analog circuit which is called an integrator. The FOH signal is reconfigured as a piecewise linear approximation of the original sampled signal. In [1], the FOH signal is used for real-time substructure testing, which is a novel method of testing structures under dynamic loading. An extrapolation of a first-order-hold discretization is used which increases the accuracy of the numerical model over more direct explicit methods. The improvements are demonstrated using a series of substructure tests on a simple portal frame. Some deep mathematical relationship between ZOH and FOH is revealed in [2-5]. It is shown that the zeros of sampled-data systems resulting from rapid sampling of continuous-time systems preceded by a ZOH are the roots of the Euler-Frobenius polynomials. The simplicity, negative realness, and interlacing properties of the sampling zeros of ZOH and FOH sampled systems are proven for the first time in literature. The paper [6] deals with the quality requirements of the synthesized sine waves reconstructed through a ZOH and FOH for testing purposes, especially when a switching demodulator is used. Results show that a FOH implies a decrease of total harmonic amplitude distortion, but the measured spurious harmonics are kept lower or equal when using a ZOH in the 15 closest components. It is concluded in the paper that in testing applications a ZOH yields better results, thus the benefits of using a FOH need further investigation. The effects of various sensing techniques on the performance of the motion canceling bilateral control (MCBC) are studied [7-9]. MCBC is a method to synchronize motion of a teleoperation robot and a target, while an operator can obtain tactile sensation of the remote target [10, 11]. Results show that a FOH yields better performance compared with a ZOH, but it has a peak gain near the Nyquist frequency. Therefore, in order to make full

use of FOH, additional techniques are needed in order to eliminate the adverse effects of the FOH. The mathematical structure of new discretization schemes are proposed and characterized as useful methods of establishing concrete connections between numerical and system theoretical properties [12-14]. The paper [15] deals with the necessary and sufficient condition for the reachability of the sampled-data system obtained by the discretization of a linear time-invariant continuous-time system with a FOH. The equivalence of the reachability and controllability of the system is shown and similar results are given for observability and re-constructability [16-19].

2. First-order Hold

The motivation in this paper is on the better estimation of the analog signal based on the digital signal $\theta_{A/D}$ read from the analog-to-digital converter (ADC). As a result, the closed-loop tracking performance could be improved. For this, the first-order-hold (FOH) is a better method to approximate the continuous analog signal than the zero-order hold (ZOH) [20]. As mentioned previously, the FOH signal is a reconstructed piecewise linear approximation to the original sampled signal (see Figure 1).

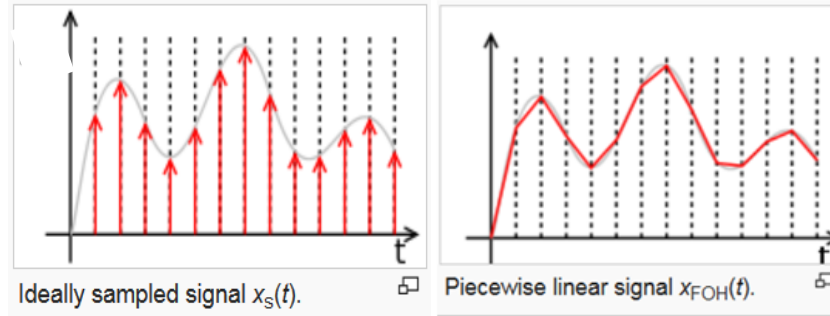


Figure 1 [21]. Ideally sampled signal and corresponding piecewise linear FOH signal.

The ideally sampled signal could be represented as,

$$x_s(t) = T \sum_{n=-\infty}^{\infty} x(nT) \delta(t - nT) \quad (1)$$

where $x(t)$ is the original signal, $x_s(t)$ is the ideal signal, $\delta(t)$ is the Dirac impulse function. Since a sequence of Dirac impulses, representing the discrete samples, is low-pass filtered, the mathematical model for FOH is necessary. The impracticality of outputting a sequence of Dirac impulses foster the development of devices that use a conventional DAC and some linear analog circuitry, to reconstruct the piecewise linear output for the FOH signals. The commonly used analytical piecewise linear approximation is written as,

$$x_{FOH}(t) = \sum_{n=-\infty}^{\infty} x(nT) tri\left(\frac{t-nT}{T}\right) \quad (2)$$

where tri is the triangular function defined as,

$$tri(t) = \max(1 - |t|, 0) \quad (3)$$

However, the system represented in (2) is not achievable in reality. In fact, the typical FOH model used in practice is the delayed first-order hold, which is identical to the FOH except for the fact that its output is delayed by one sample period, resulting in a delayed piecewise linear output signal (see Figure 2).

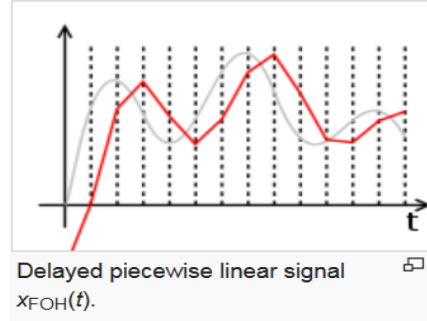


Figure 2 [21]. Delayed piecewise linear FOH signal

The delayed first-order hold, also known as causal first-order hold, as shown in Figure 2 can be represented as,

$$x_{FOH}(t) = \sum_{n=-\infty}^{\infty} x(nT) \text{tri}\left(\frac{t-T-nT}{T}\right) \quad (4)$$

The delayed output renders the system a causal system [22-25]. The corresponding delayed piecewise linear reconstruction is physically realizable with the assistance of a digital filter[26-28].

2.1 First-order Hold VS Zero-order Hold

The zero-order hold (ZOH) is a mathematical representation of the practical signal reconstruction done by a conventional digital-to-analog converted (DAC). It works in a way that the signal is held at each sample value for each and every sample interval while converting a discrete-time signal to a continuous-time signal. The most commonly used sensing feature in practice is the ZOH due to its ease of implementation [29-32]. The mathematical model of the ZOH is written as,

$$x_{ZOH}(t) = \sum_{n=-\infty}^{\infty} x[n] \text{rect}\left(\frac{t-nT}{T} - \frac{1}{2}\right) \quad (5)$$

where $x[n]$ is the discrete samples, $\text{rect}()$ is the rectangular function as follows,

$$\text{rect}(t) = \begin{cases} 0, & \text{if } |t| > 1/2 \\ \frac{1}{2}, & \text{if } |t| = 1/2 \\ 1, & \text{if } |t| < 1/2 \end{cases} \quad (6)$$

Next, the properties of the FOH and the ZOH are compared as shown in Figure 3,

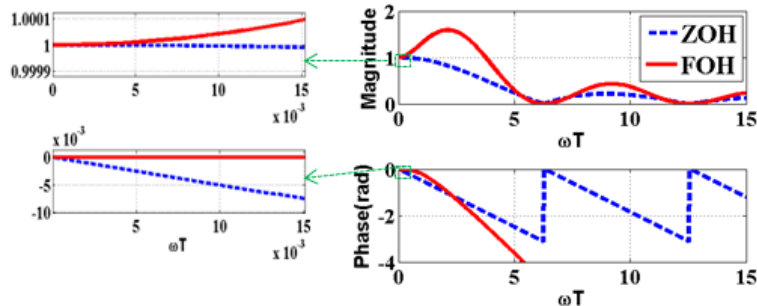


Figure 3. Magnitude and phase of ZOH and FOH filters

From Figure 3, for low frequency (below $\pi/2T$) signals, although the FOH has larger amplitude distortion than the ZOH does, the FOH has significantly less phase lag than the

ZOH does [20]. This property is utilized in this paper to reduce the level of steady state tracking error based on the fact that a more precise sensing signal is being utilized for the feedback. The details of the implementation are illustrated in the following section.

3. Implementation of the FOH on an Experimental Setup

The enhanced tracking performance while using the FOH instead of the ZOH is demonstrated over a single axis manipulator test platform (an under-actuated pendulum) as shown in Figure 4.

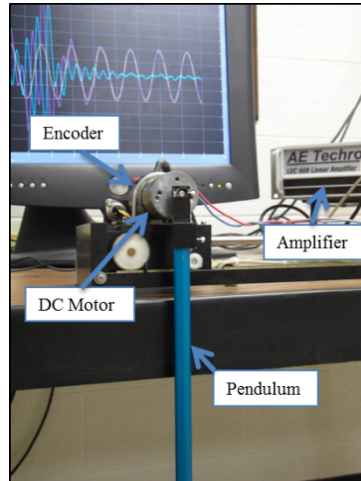


Figure 4. Experimental setup

The trajectory tracking performance of the pendulum is investigated. The desired trajectory is selected as a sinusoidal motion, for simplicity, at approximately twice the pendulum's natural frequency, that is,

$$\theta_d = 0.1 \sin(4\pi t) \text{ rad} \quad (7)$$

which is at 2 Hz frequency (about twice the natural frequency of the uncontrolled system). The feedback control loop is performed at 1000 Hz sampling speed corresponding to a sampling period $T = 0.001s$. The desired frequency 2Hz is well below $\pi/2T$ and thus is a low frequency signal compared with sampling frequency. From the inset of figure 1, the magnitudes of ZOH and FOH at the desired frequency are 0.999993 and 1.000065 respectively, both of which are very close to 1. Thus the magnitude distortions are negligible. On the other hand, the phases of ZOH and FOH at the desired frequency are -6×10^{-3} and -6×10^{-7} respectively. The FOH has significantly less phase lag (about 10 to the 4th power less) than the ZOH does. Because of the excellent phase responses, the FOH discretization has been shown to increase the accuracy of the numerical model over more direct explicit methods in the real-time substructure testing [1].

A combination of feed-forward and feedback control is implemented on the pendulum. A DC servo-motor (Minertia Motor, FB5L20E) serves as the actuator while an optical encoder (with 0.09° resolution) is used to measure the pendulum angle, θ , from its

equilibrium position [33, 34]. The control action is performed at 1000 Hz sampling rate on the pendulum that has a natural frequency of 1.1 Hz.

The linearized state space representation of the test setup is given as in [35, 36]

$$\dot{x} = Ax + \bar{B}V_a \quad (8)$$

$$x = \begin{bmatrix} \theta \\ \dot{\theta} \end{bmatrix}, \quad A = \begin{bmatrix} 0 & 1 \\ -\frac{mgl}{2J} & -\frac{b + \frac{K_b K_i}{R_a}}{J} \end{bmatrix}, \quad \bar{B} = \begin{bmatrix} 0 \\ \frac{K_i}{R_a J} \end{bmatrix}$$

where V_a is the control voltage (motor armature voltage) and the other parameters are electro-mechanical properties of the motor-pendulum assembly as listed in Table 1.

Table 1. Parameters of the experimental setup

Parameter	Value	Unit
m (pendulum mass)	0.125	kg
l (pendulum length)	0.33	m
g (gravitational constant)	9.807	m/s ²
J (rotational inertia)	0.0042	kgm ²
R _a (armature resistance)	3.4	Ω
K _b (back-emf constant)	0.0592	Vs/rad
K _i (torque constant)	0.0592	Nm/A
b (torsional damping coefficient)	0.0045	Nms/rad

In order for the pendulum to follow the desired trajectory, a control structure shown in Figure 5 is implemented with the highlighted FOH sensing block

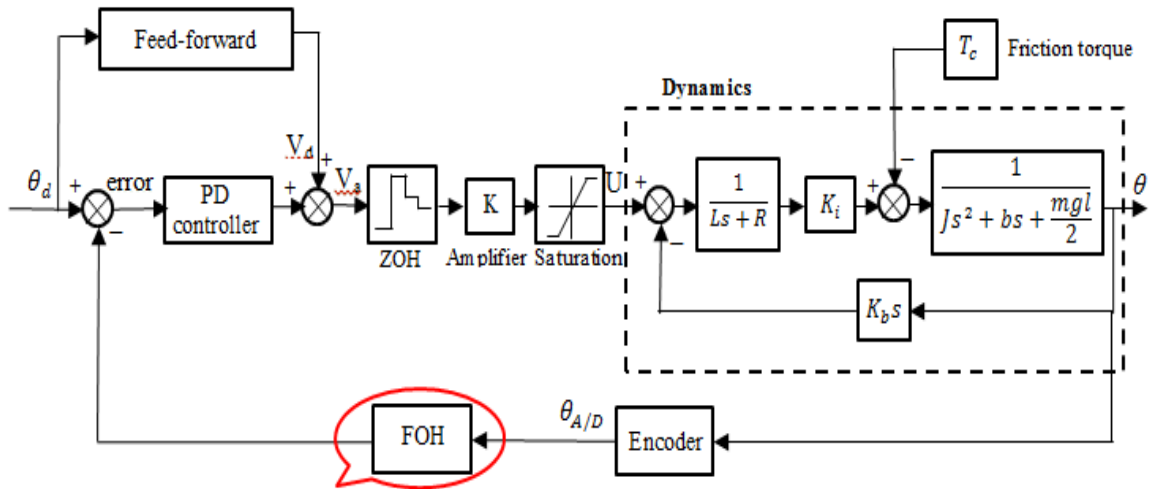


Figure 5. Block Diagram of the System Using the FOH

The feed-forward logic in the control is calculated as follows:

$$\dot{x}_d = Ax_d + \bar{B}V_d \quad (9)$$

$$V_d = \frac{R_a J}{K_i} \left(\ddot{\theta}_d + \frac{b + \frac{K_b K_i}{R_a}}{J} \dot{\theta}_d + \frac{mgl}{2J} \theta_d \right)$$

where $x_d = \begin{bmatrix} \theta_d \\ \dot{\theta}_d \end{bmatrix}$ is the desired trajectory and V_d is the feed-forward control voltage. An important point to mention is that the amplitude of θ_d should be kept small in order to maintain the linearity in (8).

Subtracting (8) from (9) gives the error dynamics as

$$\dot{e} = Ae + \bar{B}(V_d - V_a) = Ae + \bar{B}u \quad (10)$$

where $e = \begin{bmatrix} \theta_d - \theta \\ \dot{\theta}_d - \dot{\theta} \end{bmatrix}$ is the state vector describing the error, and $u = V_d - V_a = -Ke$ is the full state feedback control law.

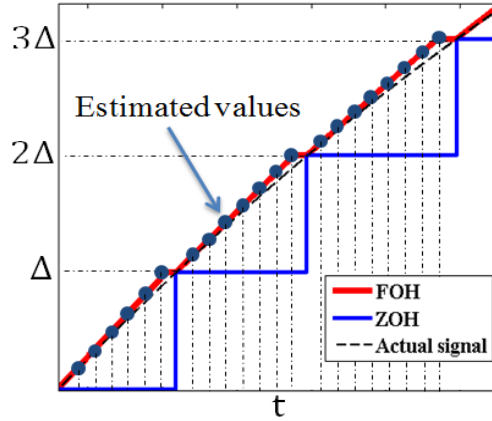


Figure 6. ZOH and FOH output signals

Figure 6 illustrates one actual signal with ZOH sampled signal and delayed FOH signal and it can be seen that the latter one yields a better approximation of the actual signal. As mentioned previously, the optical encoder with 4000 pulses per revolution has a sensor resolution Δ of 0.09 deg [37-40]. To estimate the analog signal between two quantized values, a first-order-hold (FOH) equivalent is applied to the ZOH signal $\theta_{A/D}$. The extrapolated signal is a piecewise linear approximation to the original analog signal that was sampled as shown in Figure 6. The slope of the previous step of the ZOH signal $\theta_{A/D}$ is used to estimate the output of the current step and the estimated value is obtained at the beginning of each sampling period. Since the FOH output is still not smooth enough (but yields much smaller errors in amplitude which is shown later), a second order low pass filter could be added to the FOH output.

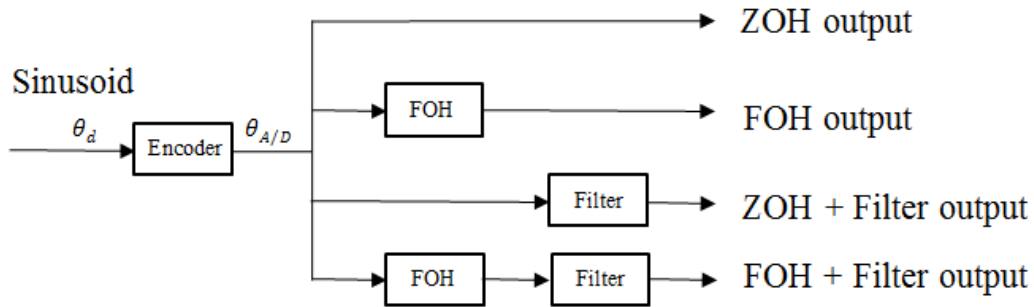


Figure 7. Comparison of various outputs with sinusoidal inputs.

Figure 7 shows various ways of sensing, i.e., ZOH, FOH, ZOH with filter and FOH with filter. In reality, a low-pass filter is usually used to eliminate high-frequency noise. The position of the FOH in the whole system is shown in Figure 5 and it is shown that the FOH is implemented for the signal obtained from the encoder. In order to compare the performance of the FOH output and ZOH output with/without the filter, a simulation is made to analyze the performance of the above methods on the sensing side as shown in Figure 7. The peak to peak errors between the various outputs and the sinusoidal input signal are obtained as listed in Table 2.

Table 2. Peak to peak error between the output of different sensing schemes and the sinusoidal input

Outputs	Peak to peak error
ZOH	1.9757%
FOH	1.6986%
ZOH+Filter	1.0135%
FOH+Filter	0.8662%

From Table 2, the FOH output yields smaller error than the ZOH output does. Also, adding a filter to the output yields apparent smaller errors than the corresponding original output. Out of all the listed methods, the filtered FOH output produces the best approximation to the continuous sinusoidal input. Based on this analysis, the closed-loop peak to peak errors with respect to different outputs on the sensing side are obtained on the simulation model (Figure 5). The highlighted FOH block is modified according to Figure 7 to get various outputs. The performance of different outputs from the peak to peak tracking error perspective is shown in the Table 3.

Table 3. Simulation result for the closed-loop peak to peak tracking error

Outputs	Closed-loop peak to peak error
ZOH	2.0286%
FOH	1.5693%
ZOH+Filter	1.0755%
FOH+Filter	0.9303%

The agreement between Table 3 and Table 2 shows that better sensing and reconstruction scheme yield smaller peak to peak tracking error. Finally, experimental results were done to verify the finding and show that the filtered FOH equivalence produces the best approximation to the continuous system out of all the methods examined (Table 4).

Table 4. Experimental result for the closed-loop peak to peak tracking error

Outputs	Closed-loop peak to peak error
ZOH	3.3404%
FOH	2.7345%
ZOH+Filter	2.2293%
FOH+Filter	2.1790%

Finally, the degree of the reduction of the closed-loop error for a simple trajectory tracking example is visualized in the discrete Fourier transformation (DFT) of the steady-state error, as depicted in Figure 8.

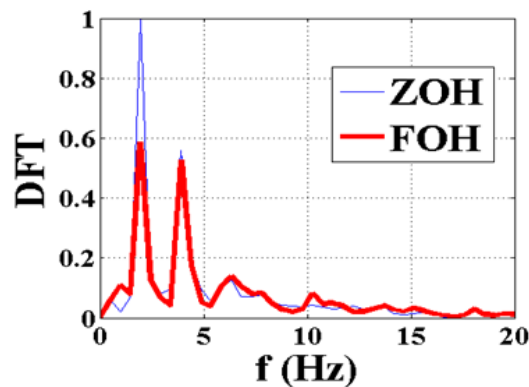


Figure 8. DFT of the closed-loop error using ZOH and FOH.

The scale of the vertical axis is normalized with respect to the maximum magnitude of the closed-loop error using ZOH sensing scheme, i.e. the ratio of $|Error_{ZOH}(\omega i)| / \max|Error_{ZOH}(\omega i)|$ expressed in percent is shown in the figure. The light line represents the DFT of the steady-state error using the ZOH sensing scheme. The bold line

depicts the DFT of the steady-state error using the FOH sensing scheme. It is observed that the dominant frequency component of 2 Hz (which is the desired frequency) is suppressed by about 40%, while the rest of the frequency spectrum remains practically unchanged.

References

- [1] A. P. Darby, A. Blakeborough, and M. S. Williams, "Improved control algorithm for real-time substructure testing," *Earthquake Engineering & Structural Dynamics*, vol. 30, no. 3, pp. 431-448, 2001.
- [2] S. R. Weller, W. Moran, B. Ninness, and A. D. Pollington, "Sampling zeros and the Euler-Frobenius polynomials," *Automatic Control, IEEE Transactions on*, vol. 46, no. 2, pp. 340-343, 2001.
- [3] Q. G. Fulai Yao, "Efficiency optimization of a power station with different generators," in *REM 2017: Renewable Energy integration with Mini/Micro grid Systems, Applied Energy Symposium and Forum 2017*, 2017.
- [4] Q. Gao, C. Dong, and H. Jia, "Multiple Time-delay Stability Analysis for the DC- Microgrid Cluster with Distributed Control," in *REM 2017: Renewable Energy integration with Mini/Micro grid Systems, Applied Energy Symposium and Forum 2017*, 2017.
- [5] Q. Gao, C. Dong, H. Jia, and Z. Zhang, "Stability Analysis for the Communication Network of DC Microgrids with Cluster Treatment of Characteristic Roots (CTCR) Paradigm," in *REM 2017: Renewable Energy integration with Mini/Micro grid Systems, Applied Energy Symposium and Forum 2017*, 2017.
- [6] A. Lozano, J. Rosell, and R. Pallas-Areny, "On the zero- and first-order interpolation in synthesized sine waves for testing purposes," *Instrumentation and Measurement, IEEE Transactions on*, vol. 41, no. 6, pp. 820-823, 1992.
- [7] Y. Nakajima, T. Nozaki, T. Mizoguchi, and K. Ohnishi, "Transparency analysis of motion canceling bilateral control under sensing constraints," ed, 2012, pp. 1-6.
- [8] Q. Gao, R. Cepeda-Gomez, and N. Olgac, "The Homicidal Chauffeur Problem with Multiple Time Delayed Feedback," *IFAC Proceedings Volumes*, vol. 45, no. 14, pp. 97-101, 2012.
- [9] Q. Gao, U. Zalluhoglu, and N. Olgac, "Equivalency of Stability Transitions Between the SDS (Spectral Delay Space) and DS (Delay Space)," in *ASME 2013 Dynamic Systems and Control Conference*, 2013, pp. V002T21A001-V002T21A001: American Society of Mechanical Engineers.
- [10] Q. Gao, R. Cepeda-Gomez, and N. Olgac, "A test platform for cognitive delays: target tracking problem with multiple time-delayed feedback control," *International Journal of Dynamics and Control*, vol. 2, no. 1, pp. 77-85, 2014.
- [11] Q. Gao, U. Zalluhoglu, and N. Olgac, "Investigation of Local Stability Transitions in the Spectral Delay Space and Delay Space," *Journal of Dynamic Systems, Measurement, and Control*, vol. 136, no. 5, p. 051011, 2014.
- [12] Z. Zheng and C. Kil To, "Comparison between first-order hold with zero-order hold in discretization of input-delay nonlinear systems," ed, 2007, pp. 2892-2896.
- [13] Q. Gao, A. S. Kammer, U. Zalluhoglu, and N. Olgac, "Sign inverting and Delay Scheduling Control concepts with multiple rationally independent delays," in *American Control Conference (ACC), 2014*, 2014, pp. 5546-5551: IEEE.
- [14] Q. Gao, A. S. Kammer, U. Zalluhoglu, and N. Olgac, "Some critical properties of sign inverting control for LTI systems with multiple delays," in *Decision and Control (CDC), 2014 IEEE 53rd Annual Conference on*, 2014, pp. 3976-3981: IEEE.
- [15] T. Hagiwara, "Preservation of reachability and observability under sampling with a first-order hold," *Automatic Control, IEEE Transactions on*, vol. 40, no. 1, pp. 104-107, 1995.
- [16] Q. Gao, A. S. Kammer, U. Zalluhoglu, and N. Olgac, "Combination of sign inverting and delay scheduling control concepts for multiple-delay dynamics," *Systems & Control Letters*, vol. 77, pp. 55-62, 2015.

- [17] Q. Gao, A. S. Kammer, U. Zalluhoglu, and N. Olgac, "Critical effects of the polarity change in delayed states within an LTI dynamics with multiple delays," *IEEE Transactions on Automatic Control*, vol. 60, no. 11, pp. 3018-3022, 2015.
- [18] Q. Gao and N. Olgac, "Dixon resultant for cluster treatment of LTI systems with multiple delays," *IFAC-PapersOnLine*, vol. 48, no. 12, pp. 21-26, 2015.
- [19] Q. Gao and N. Olgac, "Optimal sign inverting control for time-delayed systems, a concept study with experiments," *International Journal of Control*, vol. 88, no. 1, pp. 113-122, 2015.
- [20] G. F. Franklin, *Digital control of dynamic systems*, 2nd ed., repr. with corrections. ed. Reading, Mass.: Reading, Mass. : Addison-Wesley, 1994.
- [21] Wikipedia. *First-order hold*.
- [22] Q. Gao, "Stability Analysis and Novel Control Concepts for Multiple Time-delay Systems," 2015.
- [23] Q. Gao and N. Olgac, "Bounds of imaginary spectra of LTI systems in the domain of two of the multiple time delays," *Automatica*, vol. 72, pp. 235-241, 2016.
- [24] Q. Gao and N. Olgac, "Differentiability of imaginary spectra and determination of its bounds for multiple-delay LTI systems," in *Flexible Automation (ISFA), International Symposium on*, 2016, pp. 296-302: IEEE.
- [25] Q. Gao and N. Olgac, "Optimal sign inverting control for multiple time-delayed systems," in *American Control Conference (ACC), 2016*, 2016, pp. 979-984: IEEE.
- [26] Q. Gao, Z. Zhang, and C. Yang, "Sign Inverting Control and its Important Properties for Multiple Time-Delayed Systems," in *ASME 2017 Dynamic Systems and Control Conference*, 2017, pp. V001T03A004-V001T03A004: American Society of Mechanical Engineers.
- [27] Q. Gao and N. Olgac, "Stability analysis for LTI systems with multiple time delays using the bounds of its imaginary spectra," *Systems & Control Letters*, vol. 102, pp. 112-118, 2017.
- [28] R. Schmid, Q. Gao, and N. Olgac, "Eigenvalue assignment for systems with multiple time-delays," in *2015 Proceedings of the Conference on Control and its Applications*, 2015, pp. 146-152: Society for Industrial and Applied Mathematics.
- [29] F. Yao and Q. Gao, "Optimal Control and Switch in a Hydraulic Power Station," in *IEEE IAEAC 2017, Proceedings of 2017 IEEE 2nd Advanced Information Technology, Electronic and Automation Control Conference*, 2017.
- [30] F. Yao and Q. Gao, "Optimal Control and Switching Mechanism of a Power Station With Identical Generators," in *ASME 2017 Dynamic Systems and Control Conference*, 2017, pp. V001T09A006-V001T09A006: American Society of Mechanical Engineers.
- [31] Z. Zhang, N. Olgac, and Q. Gao, "An effective algorithm to achieve accurate sinusoidal amplitude control with a low-resolution encoder," in *Advanced Intelligent Mechatronics (AIM), 2017 IEEE International Conference on*, 2017, pp. 934-939: IEEE.
- [32] Z. Zhang and Q. Gao, "Characterization of Extreme Low-Resolution Digital Encoder for Control System with Sinusoidal Reference Signal," in *19th International Conference on Networking, Sensing and Control*, 2017, vol. 11, no. 5, pp. 890-896.
- [33] Z. Zhang and N. Olgac, "An Adaptive Control Method for Ros-Drill Cellular Microinjector with Low-Resolution Encoder," *Journal of medical engineering*, vol. 2013, 2013.
- [34] Z. Zhang and N. Olgac, "An Adaptive Control Method With Low-Resolution Encoder," in *ASME 2013 Dynamic Systems and Control Conference*, 2013, pp. V003T35A001-V003T35A001: American Society of Mechanical Engineers.
- [35] G. F. Franklin, J. D. Powell, and A. Emami-Naeini, "Feedback control of dynamics systems," *Pretince Hall Inc*, 2006.
- [36] Z. Zhang, J. F. Diaz, and N. Olgac, "Adaptive gain scheduling for rotationally oscillating drill, with low-resolution feedback," *International Journal of Mechatronics and Manufacturing Systems*, vol. 6, no. 5-6, pp. 397-421, 2013.
- [37] Z. Zhang, *Control Design and Analysis for Rotationally Oscillating Drill (Ros-Drill), with Low-Resolution Feedback*. University of Connecticut, 2012.
- [38] Y. Huang, Z. Zhang, C. Ji, and D. T. Phan, "Disk drive measuring stroke difference between heads by detecting a difference between ramp contact," ed: Google Patents, 2016.
- [39] S. Tang, Z. Zhang, C. Ji, and D. T. Phan, "Data storage device demodulating servo burst by computing slope of intermediate integration points," ed: Google Patents, 2016.
- [40] A. Babinski *et al.*, "Electronic system with media scan mechanism and method of operation thereof," ed: Google Patents, 2016.